Short wavelength optoacoustic spectroscopy based on water muting

Jaya Prakash[1,§], Ara Ghazaryan[1,§], Mir Mehdi Seyedebrahimi[1,§], Jaber Malekzadeh-Najafabadi[1], and Vasilis Ntziachristos[1,2,*]

[1]Institute of Biological and Medical Imaging, Helmholtz Zentrum München, Neuherberg, Germany.
[2]Chair of Biological Imaging and TranslaTUM, Technical University of Munich, Munich, Germany.

[§]Equal contribution

***Corresponding author:**

Prof. Vasilis Ntziachristos
Technical University of Munich and Helmholtz Zentrum München
Ismaningerstr 22, D-81675
Munich, Germany
Tel: +49 89 3187 3852
Email: v.ntziachristos@tum.de

Key words

Sensing, Photoacoustic, Near Infrared, Temperature, Spectrum, Glucose

Abstract

Infrared optoacoustic spectroscopy can separate a multitude of molecules based on their absorption spectra. However, the technique is limited when measuring target molecules in aqueous solution by strong water absorption at infrared wavelengths, which reduces detection sensitivity. Based on the dependence of optoacoustic signal on the temperature of the probed medium, we introduce cooled IR optoacoustic spectroscopy (CIROAS) to mute water contributions in optoacoustic spectroscopy. We showcase that spectral measurements of proteins, lipids and glucose in the short-wavelength infrared (SWIR) region, performed at 4 °C, lead to marked sensitivity improvements over conventional optoacoustic or IR spectroscopy. We elaborate on the dependence of optoacoustic signals on water temperature and demonstrate polarity changes in the recorded signal at temperatures below 4 °C. We further elucidate the dependence of the optoacoustic signal and the muting temperature on sample concentration and demonstrate that changes in these dependences enable quantification of the solute concentration. We discuss how CIROAS may enhance the abilities for molecular sensing in the infrared.

Abbreviations

Add a simple table listing all abbreviations used in the paper, e.g.

Introduction

Measurement of proteins, lipids, collagen and sugars is essential in biomedical research and diagnostics or therapeutics [1]–[7] and can lead to differentiating healthy from diseased tissues [8]–[11]. Several tissue biomolecules exhibit absorption of light in the ultraviolet (UV), visible and infrared (IR) ranges and therefore can be detected by optical spectroscopy [12], [13] (OS). Nevertheless, despite wide utilization in determining concentrations of chromophores, OS of many intrinsic tissue biomolecules comes with various disadvantages that depend on the wavelength range employed. UV wavelengths cause photo-damage in biological samples, while visible and near-infrared wavelengths provide relatively poor sensitivity for lipids, sugars and proteins [14], [15]. Longer wavelengths, such as those in the short-wave IR (900-1800 nm), offer detection of endogenous molecules such as proteins, lipids and sugars with higher contrast, but the sensitivity of the technique is limited by the absorption of water [12]–[15].

To avoid the problem of water absorption, it is common to tag target biomolecules with fluorescent labels in order to increase detection sensitivity [16]. Raman spectroscopy is also considered as it detects symmetric vibrations of nonpolar molecules and therefore is insensitive to water absorption. Although Raman spectroscopy can be performed at the UV, visible and IR wavelengths, the UV and visible regimes are heavily influenced by background auto-fluorescence in tissues [5], [17]. In fact, even weak fluorescence is much stronger than the generated Raman signal [17], which is why ultrasensitive trace detection is typically performed based on fluorescence (requires 10^{-16} cm^2/molecule) rather than Raman spectroscopy (requires 10^{-30} - 10^{-25} cm^2/molecule) [17], [18]. Therefore, longer wavelengths are preferred for Raman sensing. Nevertheless, Raman scattering by biological samples generally leads to low signal-to-noise ratios (SNRs) for detailed studies, reflecting the fact that usually only 1 in 10^{10} photons undergoes a Stokes or anti-Stokes shift [10], [17], [18]. The Raman signal can be strengthened by increasing light intensity, but this leads to photo-damage. Alternatively, significant detection improvement can be achieved by bringing molecules in close proximity to metallic nanostructures in so-called surface-enhanced Raman spectroscopy [18].

Optoacoustic spectroscopy has also been considered for characterizing a range of biologically relevant chromophores in aqueous environments, including haemoglobin, melanin or contrast agents such as gold nanoparticles and organic dyes [19]–[23] and in analytical chemistry and nanomedicine applications [24], [25]. The method detects the emission of sound waves from target molecules following absorption of incident light of transient intensity. Nevertheless, similarly to optical methods, optoacoustic sensing is limited by water absorption at longer wavelengths. Water contributes minimally to optoacoustic measurements in the visible range (450-650 nm) and near-infrared range (650-900 nm) [14], but it contributes strongly to measurements at wavelengths longer than 900 nm, limiting the sensitivity of the technique for detecting proteins, lipids, collagen and sugars [14], [26], [27].

Our goal was to develop an IR spectroscopy method that could overcome the limitations of existing Raman or IR spectroscopy implementations and improve the sensitivity and accuracy achieved in determining solute concentrations in aqueous solution. We hypothesized that we could improve the sensitivity of optoacoustic spectroscopy by minimizing the contributions of water using temperature modulation of the sample being examined. This hypothesis is based on a long known property of the thermal expansion coefficient of water, which becomes zero at 4 °C [28]. The dependence of optoacoustic signal on temperature has been experimentally demonstrated in the NIR spectral region (700-900 nm) [22], [29], [30], [31].

To investigate the validity of our hypothesis we developed the first Cooled IR Optoacoustic Spectroscopy (CIROAS) arrangement and applied it to record optoacoustic spectra of lipids, bovine serum albumin (BSA) and glucose in aqueous solution at different temperatures. For the first time, we muted water contributions in the NIR-II region (900-1900 nm), where sugars, lipids, and proteins emit strong optoacoustic signals, generally much stronger than in the NIR. Therefore, we aimed to remove the strong contributions from water on the signal collected in the NIR-II and detect these moieties with higher sensitivity. Measurements were performed over many wavelengths in the NIR-II region and compared the CIROAS detection sensitivity to conventional optoacoustic NIR-II spectroscopy at room temperature. To elucidate the CIROAS principle of operation, we studied how solute concentration influences (a) the muting point of an aqueous solution (temperature at which water signal is muted) and (b) the rate of change of optoacoustic signal with temperature. We further showcase that the rate of change of the OA signal as a function of temperature can be employed to quantitatively determine the solute concentration. We discuss how CIROAS may substantially extend the ability of optoacoustics to sense biological molecules in cells and tissues.

Methods

1. Theory

Generation of optoacoustic signal requires stress and thermal confinement criteria to be satisfied [22], [32], [33]. Thermal and stress confinement conditions can be satisfied by having the pulse width of light excitation to be shorter than thermal and stress relaxation times, respectively [32]. Once these criteria's are satisfied, the fractional volume expansion $\left(\frac{dV}{V}\right)$ generated by the pulsed laser is written as [32],

$$\frac{dV}{V} = -\kappa\Delta p + \beta\Delta T \tag{1}$$

where κ is the isothermal compressibility, β is the thermal expansion coefficient, and Δp and ΔT represent the changes in measured pressure and temperature, respectively.

When the pulse width is on the order of nanoseconds, the heating is rapid, and the accompanying fractional volume expansion is negligible (i.e. $\frac{dV}{V} = 0$); therefore the local pressure rise after the laser excitation pulse will be [32],

$$\Delta p = \frac{\beta\Delta T}{\kappa} = \frac{\beta}{\kappa\rho C_v} H = \Gamma H \tag{2}$$

where ρ is the mass density, C_v represents the specific heat capacity at constant volume, and H is the absorbed optical energy density. Furthermore, the dimensionless Grueneisen parameter (Γ) can be defined as [32],

$$\Gamma = \frac{\beta}{\kappa\rho C_v} = \frac{\beta v^2}{C_p} = g(T) \tag{3}$$

where v is the speed of sound, C_p indicates the specific heat capacity at constant pressure, and T represents temperature of the medium being probed. Therefore,

$$\Delta p = g(T)H \tag{4}$$

The pressure rise (optoacoustic signal) is a function of temperature of the object under investigation (as seen in Eq. 4). Thus prior works have used the generated optoacoustic signal during laser excitation for monitoring the temperature of the medium [34]. Given that the instantaneous temperature increase in the medium due to the laser pulse heating is of the order of milli-Kelvins [32], the laser pulse heating will not affect the Grueneisen parameter value.

Notably, the thermal expansion coefficient β is related to the temperature through the following relation [29],

$$\beta = \beta_1 + \beta_2 T \quad (5)$$

where β_1 and β_2 are the first two coefficients in a power (Taylor) series expansion of β.

Eq. 3, Eq. 4 and Eq. 5, are combined to yield,

$$\Delta p = \frac{(\beta_1+\beta_2 T)v_s^2}{C_p} H \quad (6)$$

Interestingly, $\beta_{water} = 0$ for water at 4 °C [28], [35], resulting in zero optoacoustic signal (i.e. water is optoacoustically mute). When the temperature is reduced further, β_{water} becomes negative, leading to a reversed optoacoustic signal, with the physical meaning that the optoacoustic point source first contracts and then expands upon excitation. In contrast, at temperatures above 4 °C, β_{water} is monotonic and positive, leading to generation of an optoacoustic signal with the expected bipolar signal (i.e. positive peak followed by negative peak).

The underlying CIROAS premise is that the presence of target solutes in water (such as lipids, proteins or sugars) would alter the temperature dependence of the optoacoustic signal generated by the solute compared to water, by changing the thermal expansion coefficient of the aqueous solution. The thermal expansion coefficient of the aqueous solution can be written as,

$$\beta_{aqueous} = \beta_{water} + \Delta\beta \quad (7)$$

The generated optoacoustic signal can then be written as,

$$\Delta p = \beta_{aqueous} \frac{v_s^2}{C_p} H = (\beta_{water} + \Delta\beta) \frac{v_s^2}{C_p} H \quad (8)$$

Assuming the coefficients of the Taylor series are similar in water and aqueous solution, our aim is to demonstrate that the variations in the muting point could be potentially used to measure the concentration of the sample being investigated. Notably the shift in the muting temperature of a solute vs. the muting temperature of water (i.e. 4 °C) as a function of solute concentration is given by the Despretz law, i.e. $\Delta T = Kc$, where K is the Despretz constant and c is the solute concentration[31], [36]. Here ΔT represents a small change in the temperature from 4 °C to the actual muting point in the presence of solutes. In the context of optoacoustics, we can rewrite the thermal expansion coefficient of the aqueous solution at muting temperature of solute ($T_{mute} + \Delta T$) as,

$$\beta_{aqueous} = \beta_1 + \beta_2 T = \beta_1 + \beta_2 (T_{mute} + \Delta T) = \beta_{water} + \beta_2 (\Delta T) \quad (9)$$

where T_{mute} indicates the muting point of water. Therefore at 4 °C, the optoacoustic signal from an aqueous solution is,

$$\Delta p = \beta_{aqueous} \frac{v_s^2}{C_p} H = \beta_2 \Delta T \frac{v_s^2}{C_p} H \quad (10)$$

We can rewrite Eq. 10 using Despretz Law at 4 °C as,

$$\Delta p = \beta_2 K c \frac{v_s^2}{C_p} H \quad (11)$$

Eq. 11 indicates that the optoacoustic pressure detected at water muting temperature is proportional to the solute concentration and can be therefore used for quantitative spectroscopy purposes. We were particularly interested herein in identifying the use of Eq. 11 in the SWIR spectral region. Quantifying the changes in the optoacoustic signal intensity at SWIR excitation wavelengths at which the solute target strongly absorbs, under water muting conditions, could allow an accurate determination of target concentration with higher sensitivity than in the NIR.

2. Experimental Setup

The CIROAS system (Fig. 1) employed the illumination of a tuneable nanosecond SpitLight Single OPO laser (Innolas, Krailling, Germany). The output power was set to 0.5 mJ across the whole NIR-II spectral range of 900 – 1900 nm. The wavelength scanning step was set to 10 nm. A cylindrically focused ultrasonic transducer (UST) with 7.5 MHz central frequency (V319, Olympus Panametrics-NDT, Tokyo, Japan) was used for detecting the generated optoacoustic signal. The UST was adjusted to accommodate the beam in its focus. Acquired signals first were amplified with a low noise amplifier, AMP (AU-1291, Miteq Inc., USA), then digitized using a fast data acquisition card (DAQ) operating at 100 MS/s (EON-121-G20, Gage-applied, Lockport, IL). Simultaneously, the intensity of light passed through medium was registered by power meter and the values were used to calculate the optical absorption. A trigger signal from the photodiode (PD) was used to synchronize the detection in DAQ. To measure OA spectra at different temperatures a measurement chamber was built, where temperature was controlled using Peltier elements (Fig. 1). Six thermocouple-based temperature sensors were placed inside the chamber to provide accurate reading of the temperature. The average value of measured temperature was used in closed-loop configuration to control the Peltier Elements, maintaining the desired temperature. During all measurements, a mechanical stirrer was constantly mixing the solution to ensure homogeneous temperature throughout the measurement chamber.

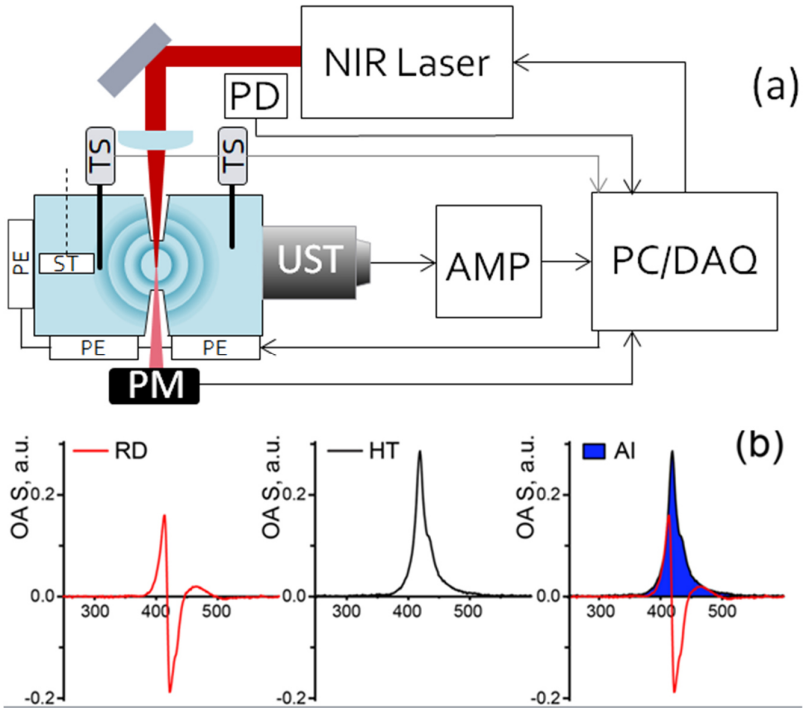

Fig. 1 **a**) Schematic representation of the experimental setup for optoacoustic spectroscopy. UST – ultrasound transducer; PD – photodiode; AMP – amplifier; TS – temperature sensor; PM – power meter; ST – stirrer; PE – Peltier Element; PC/ DAQ

– personal computer with data acquisition card **b**) Data processing and analysis steps. OAS raw data (RD, left) was transformed by Hilbert transformation (HT, middle), and the area of interest (AI, right – in blue) under curves was taken as the intensity of the OAS signal (I_{OA}).

Data collection and processing

Data acquisition and processing were performed in MATLAB (Mathworks, Natick, MA). Obtained raw signal intensities were normalized per laser energy as registered by powermeter. The strength of the optoacoustic signal (I_{OA}) was estimated by computing the Hilbert transform of the recorded acoustic signal of each measurement and integrating the area under the curve (Fig. 1b) as previously suggested [27]. For each wavelength, 40 optoacoustic measurements were recorded and averaged to increase SNR.

3. Experimental Measurements.

To examine the merits of Cooled IR Optoacoustic Spectroscopy (CIROAS) we performed measurements of an aqueous solution at different temperatures ranging from 1.4-25.8 °C, using 1440 nm illumination. The raw optoacoustic signals and the muting temperature were recorded in these experiments. Then we examined the CIROAS ability to measure glucose in NIR-II region, as an application example. We investigated if glucose detection could be improved over conventional SWIR spectroscopy, by reducing the temperature of the medium being investigated. For this reason we prepared a stock solution of D(+)Glucose ($C_6H_{12}O_6$, Merck, Darmstadt, Germany) in distilled H_2O and added it to the test chamber in 5 titrations, covering a concentration range of 0-452 mg/dL. The test chamber contained 14 ml distilled H_2O. With each step of titration, aliquots of 1 ml of solution was first dispensed into the test reservoir, followed by addition of 1 ml of a concentrated glucose stock solution. As a second application example, we repeated the measurement with lipid solution, which was prepared by mixing intralipid (20% emulsion, I141-100ML; Sigma) in water to result in a concentration of 10% by volume (mimicking tissue scattering properties) [14]. Finally, a third example demonstration was investigated by using bovine serum albumin (BSA) solution in a concentration of 50 g/L, which is a physiologically relevant protein concentration.

Results

We investigated the optoacoustic signal detected from water as a function of temperature. We were particularly interested to study the muting property in water measured at the SWIR spectral window and to confirm our hypothesis that CIROAS of biomolecules in this wavelength range can offer accurate detection with increased sensitivity over regular spectroscopy. Fig. 2a shows the dependence of the optoacoustic signal on temperature, using illumination at 1440 nm, and depicts a decline of intensity with reducing temperature until the signal becomes undetectable (mute) at 4 °C. Further reduction in temperature leads to the appearance of optoacoustic response, however with an inverted profile (Fig. 2b; signal at 1.8 °C): i.e. the negative peak precedes the positive one for signals recorded at temperatures below 4 °C, in contrast to signals collected above 4 °C (Fig. 2c; signal at 21 °C). Fig. 2d presents the optoacoustic spectrum recorded at different temperatures from water at illumination wavelengths in the range of 900-1840 nm. At 4 °C, the entire spectrum is near baseline, as expected, indicating that water becomes optoacoustically mute in the SWIR region despite its strong absorption in this wavelength range. These measurements therefore report on the change of polarity of the optoacoustic signal for temperatures below 4 °C and the muting of the optoacoustic response in the SWIR.

Fig. 2e depicts optical and optoacoustic signals recorded from pure water at the temperature range of 1.4-25.8 °C, using 1440 nm illumination. The optical signal was recorded as an attenuation signal in transmission mode and is plotted as an absorption curve using the Beer-Lambert law. The change

of water absorption recorded with the optical measurement exhibits a minor slope of 0.001/°C with temperature. In contrast, the optoacoustic signal changes significantly (slope = 0.02/°C). This graph confirms the potential advantage of using optoacoustic spectroscopy over optical spectroscopy at reduced temperature. In particular, strong water absorption in the SWIR can overshadow the contributions from the absorption of other molecules in a solution. However, using the water muting property in the SWIR, it is possible to significantly reduce the contributions of water on the optoacoustic signal. Consequently, we then investigated whether the detection sensitivity of cooled optoacoustic spectroscopy could be increased for sensing optically absorbing molecules in aqueous solution at 4 degrees, over conventional optical spectroscopy.

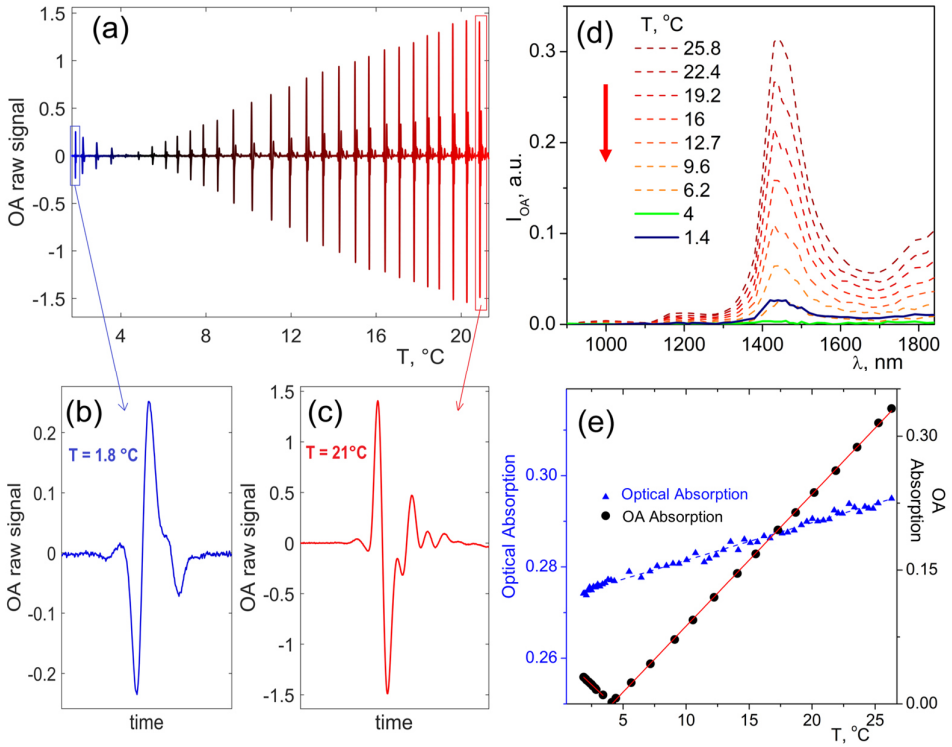

Fig. 2. Optoacoustic signal of pure water at different temperatures after illumination in the SWIR range. (a) Raw optoacoustic signal of water at different temperatures after illumination at 1440 nm. (b) Temporal raw optoacoustic signal at 1.8 °C. (c) Temporal raw optoacoustic signal at 21 °C. (d) Optoacoustic spectra of water at different temperatures after illumination in the SWIR range. (e) Comparison of the signal obtained from pure water at different temperatures after illumination at 1440 nm using optical and optoacoustic measurements.

Following the comparison between optical and optoacoustic measurements, we examined the CIROAS application to measuring solutes (Fig. 3). Fig. 3a shows the raw optoacoustic signal recorded from an aqueous solution of glucose (452.2 mg/dL) after illumination at 1580 nm as a function of temperature ranging from 0.6 to 18.5 °C. The inset in Fig. 3a zooms in the signal at 4 degrees and allows a first insight that the muting point of the glucose solution is shifted at lower temperatures than 4 °C, i.e. lower than the muting point for pure water. This observation is better shown in Fig. 3b, which plots the raw optoacoustic signals measured at 1580 nm from pure water and aqueous solution of glucose at approximately 4 °C. We observe that, in contrast to pure water, the glucose solution shows detectable optoacoustic signal at 4 °C with normal polarity, due to the change in thermal expansion coefficient of the water in the presence of solutes such as glucose, lipid or proteins.

We then examined the relative spectra measured at 4 °C from pure water and from the glucose aqueous solution at 452.2 mg/dL glucose concentration. Fig. 3c shows the optoacoustic SWIR spectra measured and demonstrated that while the pure water spectrum is close to baseline (as also shown in Fig. 2), the spectrum from the glucose aqueous solution yields a stronger signal as seen in the graph. Further, to examine whether cooling improves the detection characteristics of glucose over room temperature we plotted normalized OA spectra of water at 18 °C and of aqueous solution of glucose at 18 °C. (Fig.3d). The comparison reveals that there are differences between the pure water and glucose solution spectra especially at 1550-1700 nm spectral window. Fig. 3d indicates that the spectra of water and glucose at 18 °C are very similar, due to the strong contribution of the water absorption. However, when we compare the spectrum of water and aqueous solution of glucose at 4 °C, we observe the characteristic difference at the 1550-1700 nm spectral window also seen in Fig. 3c. Fig. 3e shows the optoacoustic spectra of aqueous solutions of glucose recorded at different temperatures. Consistent with the preliminary observation in Fig. 3a, we see that the aqueous solution of glucose gives appreciable signal at 4 °C with a maximum at approximately 1460, whereas pure water gives negligible signal (see Fig. 2d). Further, we can observe in Fig. 3e that the acquired OA spectrum goes to the baseline (close to 0, indicated in green colour) at 3.1 °C, which means the muting point has shifted to lower temperature than 4 °C. Fig. 3e also indicates that substantial OA signal was detected when temperature was further reduced to 1.5 °C, which is indicated in blue colour.

Finally, Fig. 3f shows the absolute normalized spectral difference i.e.

$$abs\left(\frac{x_{gluc}}{\max(x_{gluc})}-\frac{x_{water}}{\max(x_{water})}\right)$$

where x_{water} is the OA spectrum from pure water and and x_{gluc} is OA spectrum from glucose solution (452.2 mg/dL) at 18, 10, and 4 °C. The graph shows that CIROAS becomes more sensitive to the presence of glucose by reducing the temperature. Further, we repeated the experiment to check if the recorded OA spectrum from aqueous solution of glucose in Fig. 3c,d can be reproduced, and the corresponding result is included as Supplementary Fig. S1, which shows the normalized OA spectrum corresponding to pure water at 25 °C, glucose solution (400 mg/dL) at 4 °C, and saturated glucose solution (prepared by continuously adding glucose in heated water until the glucose does not dissolve any more). Clear difference between pure water spectrum and glucose solution spectrum at 1550-1700 nm spectral window can be seen in Fig. S1, this is similar to the result reported in Fig. 3c,d. Interestingly, the OA spectral measurements at 1550-1700 nm spectral window in Fig. S1 reveals that at higher concentration (i.e. saturated glucose) the deviation in normalized OA signal is higher compared to measurements of glucose solution at physiological concentration (i.e. 400 mg/dL and 4 °C).

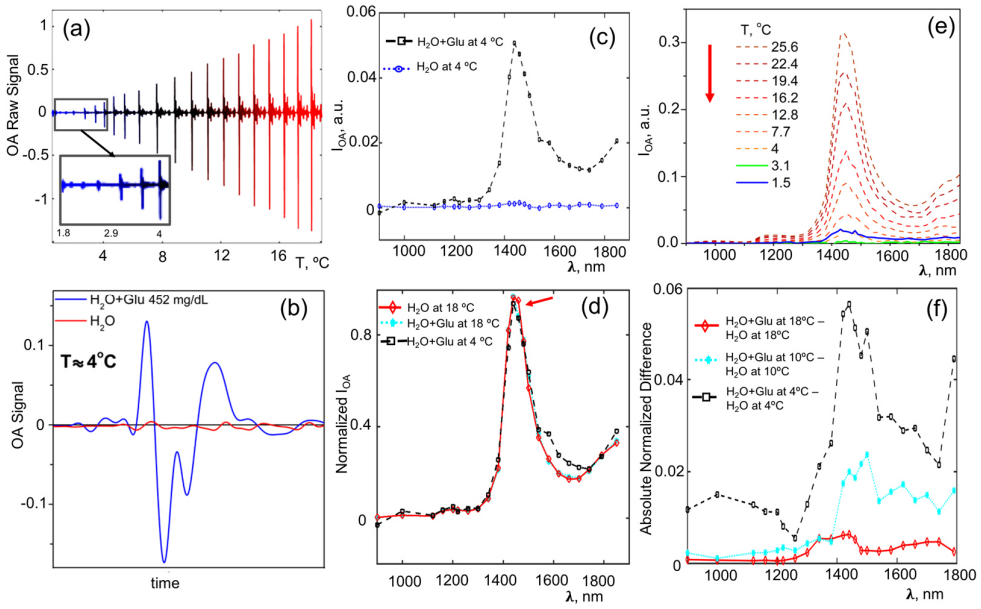

Fig. 3 Optoacoustic signal of an aqueous solution of glucose (452.2 mg/dL) at different temperatures after illumination in the SWIR range. (a) Raw optoacoustic signal at temperatures between 0.6 and 18.5 °C after illumination at 1580 nm. (b) Superposition of the optoacoustic signals of pure water (red line) and the aqueous solution of glucose (blue line) at 4 °C. (c) Optoacoustic spectra of pure water at 4 °C (dotted blue line) and the aqueous solution of glucose (dashed black line) at 4 °C. (d) Normalized optoacoustic spectra of pure water (solid red), aqueous solution of glucose at 18 °C (dotted cyan) and aqueous solution of glucose at 4 °C (dash black). (e) Optoacoustic spectra of the aqueous solution of glucose at different temperatures after illumination in the SWIR range. (f) Absolute normalized difference in OA signal recorded from an aqueous solution of glucose and water at 4 °C, 10 °C, and 18 °C.

As a next step, we examined whether changing the glucose concentration alters the muting point and the OA signal dependence on temperature. Such dependence would be in analogy to how solute concentration changes the boiling, or the freezing temperature point relative to the value for pure solvent. We performed measurements with glucose solutions in water ranging in concentration from 50 to 600 mg/dL. Representative data at 149.6 and 452.2 mg/dL are shown in Fig. 4, and illustrate a temperature dependence of the OA signal intensity at 1580 nm for pure water and for aqueous solutions of glucose. Overall, the range examined covers normal and hyperglycemic levels reported in brain and blood [3], [37], [38]. Linear fits to data show monotonic increases with temperature. The fitted lines intersect with the temperature axis at 4 °C for pure water, 3.7 °C for water containing glucose at 149.6 mg/dL and 3.1 °C for water containing glucose at 452.2 mg/dL. The corresponding slopes of fitted lines were 0.0582, 0.0538 and 0.0527. These results indicate that both the temperature intercept and OA signal-temperature slope varied proportionally with glucose concentration. This dependence can be employed for quantifying the concentration of biomolecules in solutions.

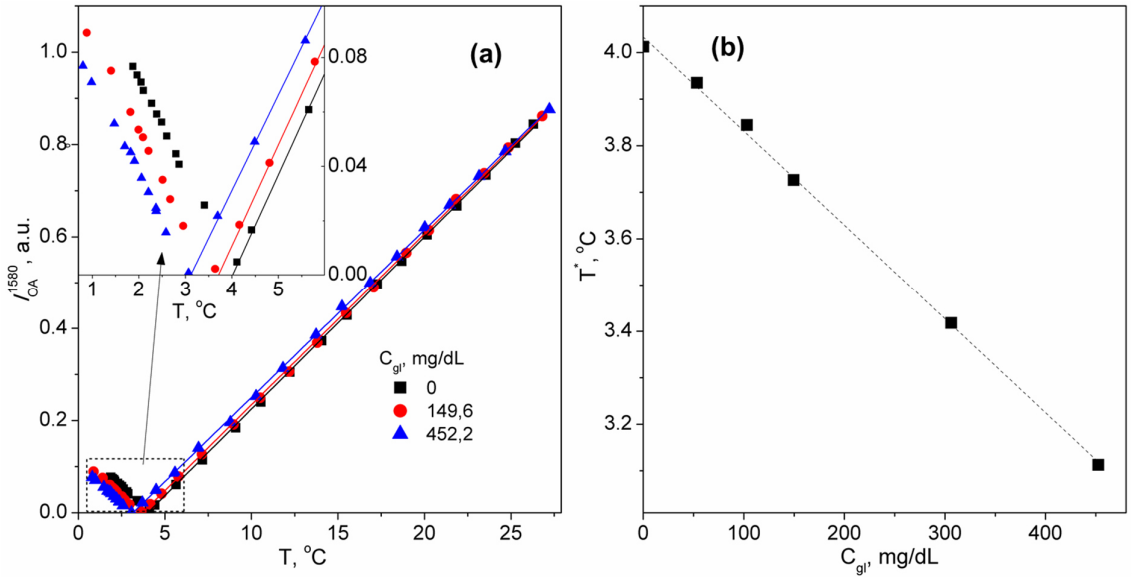

Fig. 4 Variation in the temperature dependence of optoacoustic signal from water and its "muting point" as a function of solute concentration. (a) Temperature dependence of optoacoustic signal intensity of pure water (black squares) and aqueous solutions of glucose at 149.6 mg/dL (red circles) or 452.2 mg/dL (blue triangles). Linear fitting of monotonically increasing signals is shown. The inset shows the muting point of each solution, defined as the intersection with the temperature axis. (b) Variation in muting point (T*) with glucose concentration (C_{gl}).

We further examined CIROAS of lipid and protein detection compared to measurements at room temperature. Fig. 5a shows measured OA spectra from 890 nm to 1000 nm for aqueous solution of lipids at different temperatures. This wavelength range was chosen because lipid shows a distinct peak at 930 nm, while water shows a peak at 970 nm. We observe that the 930 nm peak becomes visible at lower temperatures, but it is not prominent as we increase the temperature. We also observed that the OA signal continues to decrease as the temperature reduces below 4 °C. This signal decrease might be due to interference and OA signal cancellation between lipid (positive peak preceding negative peak below 4°C) and water (negative peak preceding positive peak below 4 °C). Note that similar behaviour was not observed while probing glucose solution, this may be because glucose is readily soluble in water compared to lipid molecules causing interference of the OA signals from lipid and water. Fig. 5b indicates the normalized OA measurements (i.e. $\frac{x}{\max(x)}$, where x is the acquired OA spectrum) from lipid solution at 19 °C and 4 °C, showing the spectral difference of the lipid solution at the two temperatures. Fig. 5c depicts the ratio of the measured OA signal at 930 nm to that of 970 nm as a function of temperature for the measurements shown in Fig. 5a. The curve shows that the relative signal obtained primarily due to lipid contributions at 930 nm becomes 4x stronger at lower temperatures compared to the signal obtained at 970 nm, which is primarily attributed to water absorption. This observation suggests a 4x lipid detection sensitivity improvement at lower temperatures.

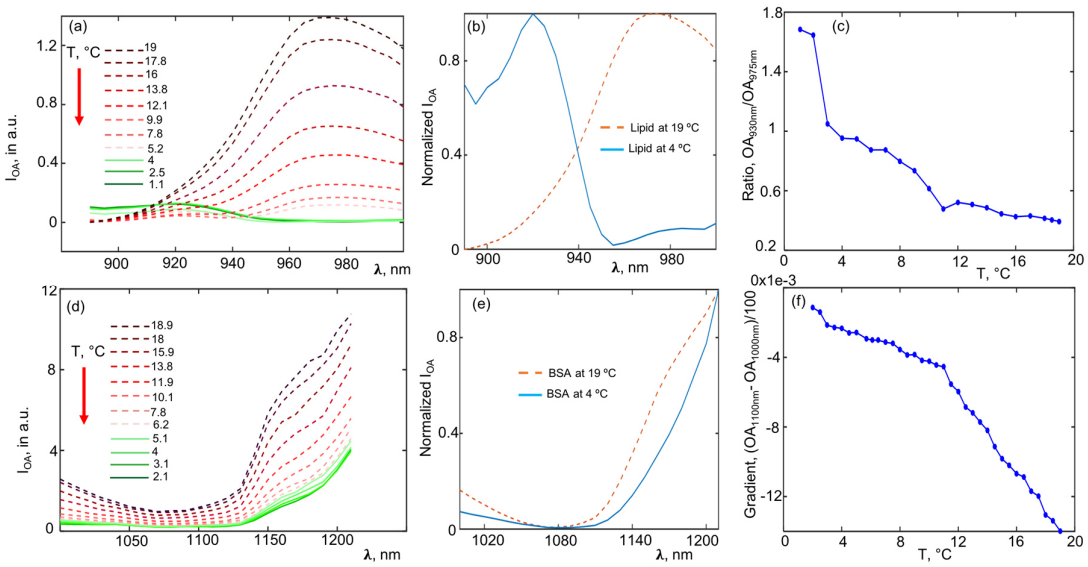

Fig. 5 Optoacoustic signal of an aqueous solution of lipid (10%) and BSA (50 g/L) at different temperatures after illumination in the SWIR range. (a) Optoacoustic spectra of lipids in aqueous solution at different temperatures after illumination in the wavelength range of 890-1000 nm. (b) Comparison of normalized OA spectra of lipid solution at 19 °C (dotted orange line) and at 4 °C (solid blue line). (c) Ratio of optoacoustic signal from the lipid solution at 930 nm (lipid peak) to signal at 970 nm (water peak) at different temperatures. (d) Optoacoustic spectra of BSA in aqueous solution at different temperatures after illumination in the wavelength range of 1000-1210 nm. (e) Comparison of normalized OA spectra of BSA solution at 19 °C (dotted orange line) and at 4 °C (solid blue line). (f) Gradient in the measured optoacoustic signal from BSA solution between 1000 and 1100 nm at different temperatures.

Fig. 5d indicates the measured OA spectra from 1000-1210 nm for an aqueous solution of BSA at different temperatures. BSA does not exhibit characteristic peaks in the measured wavelength range, but between 1000 and 1100 nm BSA shows a roughly constant absorption, whereas water decreases in absorption with increasing wavelength. Therefore, at lower temperatures, we clearly see a decrease in OA signal intensity and a flattening of the spectrum in the 1000 nm - 1100 nm range, reflecting the water muting effects. Fig. 5e plots the normalized measurements from BSA solution at 19 °C and 4 °C, showcasing the spectral differences at the two temperatures. At 4 degrees, the BSA solution shows a reduced signal compared to 18 degrees, due to the reduction of water absorption contribution to the OA signal.

An analysis similar to the one performed in Fig. 5c shows that the gradient of the optoacoustic signals obtained between 1000 nm and 1100 nm from the BSA solution similarly increases with reducing temperature. The gradient used in Fig. 5f is calculated using $\frac{y_{1100}-y_{1000}}{100}$, where y_{1100} is the OA signal from BSA solution at 1100 nm, y_{1000} is the OA signal from BSA solution at 1000 nm. Note that we used a ratio of spectral peaks for the lipid measurement (Fig. 5c) since the lipids have a distinct peak at 930 nm, whereby water at 970 nm. However, we used the gradient calculation in Fig. 5f, since the BSA spectrum does not have such distinct peaks in its spectrum. The gradient measure tends to be closer to 0 at lower temperatures, indicating that BSA spectral signature dominates at lower temperatures, but water contributions begin to appear with increasing temperature. The BSA detection sensitivity is 5 times greater at lower temperatures, compared to higher temperatures.

We also examined the muting points for lipid and protein. In contrast to the glucose measurements, whereby the muting point was same at all wavelengths, Figs S2 (a) and (b) show that the muting point of lipid solution was higher at 930 nm (i.e. about 8 °C) compared to 970 nm (where muting

point was at 2.5 ˚C. Moreover, Fig. S2(c) shows the muting point of BSA solution at 1070 nm, found to be at 1.8 ˚C, however the OA signal at higher wavelengths did not mute at all as can be seen from Fig. 5(d). Currently we investigate the variation of thermal expansion coefficient as a function of temperature for biomolecules such as glucose, lipids and proteins in order to gain better insights into these muting point variations, along the lines of Eqs 9 and 10.

Discussion

We exploited the dependence of optoacoustic signals on temperature for improving the sensitivity of infrared spectroscopy and demonstrated a 5-fold sensitivity improvement in the SWIR. We explored the modifications of the muting point as a function of solute concentration and measured OA signal as a function of temperature for a carbohydrate, a protein and a lipid solution. Previously, temperature-dependence of the optoacoustic signal have been utilized for determining the temperature of a sample; for example during thermal therapy using focused ultrasound [39], [40] or while ablating tissue with a laser fibre [34], [41]. This dependency has also been used to discriminate nonlinear optoacoustic emission of gold nanospheres dissolved in water from the linear optical absorption of the water solvent in the NIR-I region [42]. However, the effects of muting water responses at about the 4 degrees Celsius temperature has not been previously been explored. By exploiting this muting property, we show therefore a new spectroscopic approach and demonstrate benefits in utilizing optoacoustic readings over conventional optical readings, common in IR spectroscopy.

Our demonstration and analysis focused on the IR wavelengths, and in particular in the SWIR range, and addresses the long-standing problem of strong light absorption by water in this spectral region, that challenges the detection sensitivity. Moreover, it has been particularly difficult to detect metabolites such as glucose, since both water and glucose molecules have the O-H group, giving rise to a similar spectrum with a strong absorption peak at 1440 nm. By lowering the temperature and muting the contributions of water, we enable more sensitive spectroscopic detection of glucose and possibly other biomolecules, as elaborated in Figs 3-5.

We provide evidence that the “muting point” can be observed at all SWIR wavelengths and represents an essential CIROAS feature that allows up to 5-fold improved sensitivity in biomolecule detection compared to room-temperature spectroscopy. For the glucose solution, the exact muting point and the slope of thermal dependence of optoacoustic signal were shown to depend on glucose concentration. This trend could be modelled by assuming a thermal expansion coefficient β that depends on solute concentration (see Eq. 10 and Eq. 11) analogously to other colligative properties of water, such as boiling point, freezing point and vapor pressure [43], [44]. We show that the dependence of muting point on the solute concentration can be employed to quantify the concentration of biologically relevant solutes, i.e. CIROAS measurements at different temperatures can be employed for quantifying the concentration of solutes in aqueous solutions. The results further show that besides glucose, CIROAS improves the sensitivity of detection of protein and lipid, which opens up the possibility of improving detection of many other biomolecules, such as lactose, sucrose, galactose, cathepsin, integrin, and myosin. Optoacoustic measurements in the SWIR spectral range are unaffected by other abundant, but weakly absorbing chromophores such as hemoglobin and melanin, making CIROAS an attractive method for measurements of metabolites in solution.

CIROAS involves changing the temperature, which alters the speed of sound [45], [46] and thereby changing the calculated position of the optoacoustic source. However, the change in position should not pose a problem for quantitation of solutes in homogeneous solution. Nevertheless, accurate determination of the speed of sound may be useful, especially since it can allow an estimation of

sample temperature [47] during solute quantification or spectral analysis, or in imaging applications [48]. CIROAS appears to be superior to alternative optical spectroscopic methods that use heavy water as the means to overcome the effects of strong water absorption [8]. Besides being impractical and cost-ineffective, the use of heavy water is not compatible with measuring biological samples that consist of >80% of water.

Broad implementation of CIROAS will require hardware that allows the variation of the temperature of the sample, using a Peltier element or other means. Such implementations are widely available, and they do not represent a technological barrier. Therefore, CIROAS can enable a new spectroscopic approach with high dissemination potential offering a straightforward way to improve the sensitivity of detection of various molecules in biological samples. The method can be employed for conventional laboratory measurements or for analysing biological fluids, such as blood measurements. Miniaturization of components is also technically straightforward which implies applications in conventional spectroscopy or as part of micro-fluidic and lab on a chip measurement setup. In the future, imaging implementations using two- or three-dimensional optoacoustic scans can be also contemplated.

Acknowledgements

J.P. acknowledges support from Alexander von Humboldt postdoctoral fellowship program. VN acknowledges SENSE4LIFE project funded by BMBF and the Horizon 2020 INNODERM funding program.

References

[1] P. Libby, P.M. Ridker, and A. Maseri, Circulation **105**, 1135 (2002).
[2] L.S. Eberlin, I. Norton, A.L. Dill, A.J. Golby, K.L. Ligon, S. Santagata, R. Graham Cooks, and N.Y.R. Agar, Cancer Res. **72**, 645 (2012).
[3] N. Marty, M. Dallaporta, B. Thorens, and B. Thorens, Physiology **22**, 241 (2007).
[4] American Diabetes Association, Diabetes Care **34 Suppl 1**, S62 (2011).
[5] E. B. Hanlon *et al.*, *Physics in Medicine and Biology*, vol. 45, no. 2. (2000).
[6] A. Glinzer, X. Ma, J. Prakash, M.A. Kimm, F. Lohöfer, K. Kosanke, J. Pelisek, M.P. Thon, S. Vorlova, K.G. Heinze, H.-H. Eckstein, M.W. Gee, V. Ntziachristos, A. Zernecke, and M. Wildgruber, Arterioscler. Thromb. Vasc. Biol. **37**, (2017).
[7] X. Ma, V. Phi Van, M.A. Kimm, J. Prakash, H. Kessler, K. Kosanke, A. Feuchtinger, M. Aichler, A. Gupta, E.J. Rummeny, M. Eisenblätter, J. Siveke, A.K. Walch, R. Braren, V. Ntziachristos, and M. Wildgruber, Neoplasia (United States) **19**, (2017).
[8] Q. Cao, N.G. Zhegalova, S.T. Wang, W.J. Akers, and M.Y. Berezin, J. Biomed. Opt. **18**, 101318 (2013).
[9] G. Hong, S. Diao, J. Chang, A.L. Antaris, C. Chen, B. Zhang, S. Zhao, D.N. Atochin, P.L. Huang, K.I. Andreasson, J. Calvin, H. Dai, C. Division, and M.G. Hospital, **8**, 723 (2016).
[10] R. Pandey, S. Paidi, *et al.*, *Acc. Chem. Res.*, **50**, 264, (2017).
[11] K. Weinger, A.M. Jacobson, M.T. Draelos, D.M. Finkelstein, and D.C. Simonson, Am. J. Med. **98**, 22 (1995).
[12] H. W. Siesler, Y. Ozaki, and S. Kawata, *Near-Infrared Spectroscopy. Principles, Instruments, Applications*, vol. 16, no. 12. (2002).
[13] P. Larkin, *Infrared and Raman Spectroscopy; Principles and Spectral Interpretation*. (2011).
[14] A. T. Buss, N. Fox, D. A. Boas, and J. P. Spencer, *Neuroimage*, vol. 85, pp. 314–325, (2014).
[15] S.L. Jacques, Phys. Med. Biol. **58**, R37 (2013).
[16] G. A. Wagnières, W. M. Star, and B. C. Wilson, *Photochemistry and Photobiology*, vol. 68, no. 5. pp. 603–632, (1998).
[17] R. L. Mccerry, *Raman spectroscopy in chemical bioanalysis.*, vol. 8, no. 5. (2000).

[18] K. Kneipp *et al.*, *Chem. Rev.*, vol. 99, no. 10, pp. 2957–76, (1999).
[19] V. Gujrati, A. Mishra, and V. Ntziachristos, Chem. Commun. **53**, 4653 (2017).
[20] J. Laufer, D. Delpy, C. Elwell, and P. Beard, Phys. Med. Biol. **52**, 141 (2007).
[21] A.C. Tam, Rev. Mod. Phys. **58**, 381 (1986).
[22] A. Rosencwaig, Science (80-.). **181**, 657 (1973).
[23] G.P. Luke, S.Y. Nam, and S.Y. Emelianov, Photoacoustics **1**, 36 (2013).
[24] T. A. Filimonova, D. S. Volkov, M. A. ProskurninIvan, and M.Pelivanov, Photoacoustics **1**, 54 (2013).
[25] L. O. Usoltseva, D. S. Volkov, D. A. Nedosekin, M. V. Korobov, M. A. Proskurnin, and V. P. Zharov, Photoacoustics **12**, 55 (2018).
[26] J. Kottmann, J.M. Rey, J. Luginbühl, E. Reichmann, and M.W. Sigrist, Biomed. Opt. Express **3**, 667 (2012).
[27] A. Ghazaryan, M. Omar, G.J. Tserevelakis, and V. Ntziachristos, Biomed. Opt. Express **6**, 3149 (2015).
[28] G. S. Kell, J. Chem. Eng. Data, **12**, pp. 66–69, (1967).
[29] I.G. Calasso, W. Craig, and G.J. Diebold, Phys. Rev. Lett. **86**, 3550 (2001).
[30] C. Li and L. V Wang, Phys. Med. Biol. **54**, R59 (2009).
[31] E. Petrova, A. Liopo, A. A. Oraevsky, and S. A. Ermilov, *Photoacoustics*, vol. 7, pp. 36–46, (2017).
[32] L. V. Wang and Hsin-I Wu, *Biomedical Optics: Principles and Imaging* (2012).
[33] P. Beard, Interface Focus **1**, 602 (2011).
[34] E. Bay, A. Douplik, and D. Razansky, Lasers Med. Sci. **29**, 1029 (2014).
[35] M. F. Cawley, D. McGlynn, and P. A. Mooney, *Int. J. Heat Mass Transf.*, vol. 49, no. 11–12, pp. 1763–1772, 2006.
[36] M. V. Kaulgud and W. K. Pokale, *J. Chem. Soc. Faraday Trans.*, vol. 91, no. 6, pp. 999–1004, 1995.
[37] G. Freckmann *et al.*, *J. diabetes Sci. Technol.*, vol. 1, no. 5, pp. 695–703, (2007).
[38] A. J. Rose and E. a Richter, *Physiology (Bethesda).*, vol. 20, no. 131, pp. 260–270, (2005).
[39] M. Kuniyil Ajith Singh and W. Steenbergen, Photoacoustics **3**, 123 (2015).
[40] Y. Sun and B. O'Neill, Appl. Opt. **52**, 1764 (2013).
[41] G.A. Pang, E. Bay, X.L. Dean-Ben, and D. Razansky, J. Cardiovasc. Electrophysiol. **26**, 339 (2015).
[42] O. Simandoux, A. Prost, J. Gateau, and E. Bossy, Photoacoustics **3**, 20 (2014).
[43] F.C. Andrews, Science, **194**, 567 (1971).
[44] G. S. Manning, J. Chem. Phys., **51**, 3249 (1969).
[45] J. Jose, R.G.H. Willemink, W. Steenbergen, C.H. Slump, T.G. van Leeuwen, and S. Manohar, Med. Phys. **39**, 7262 (2012).
[46] S. Mandal, E. Nasonova, X.L. Deán-Ben, and D. Razansky, Photoacoustics **2**, 128 (2014).
[47] D. de Sompel, L.S. Sasportas, A. Dragulescu-Andrasi, S. Bohndiek, and S.S. Gambhir, PLoS One **7**, e45337 (2012).
[48] I. Steinberg, D. M.Huland, O. Vermesh, E. Frostig, W. S.Tummers, and S. S.Gambhir, Photoacoustics, *in press*(2019).